

# Production of Au–Ag alloy nanoparticles by laser ablation of bulk alloys

Inhyung Lee, Sang Woo Han and Kwan Kim\*

Laboratory of Intelligent Interface, School of Chemistry and Molecular Engineering and Center for Molecular Catalysis, Seoul National University, Seoul 151-742, Korea.

E-mail: kwankim@plaza.snu.ac.kr

Received (in Cambridge, UK) 20th June 2001, Accepted 6th August 2001

First published as an Advance Article on the web 3rd September 2001

**Gold–silver alloy nanoparticles can be produced by pulsed laser irradiation of bulk alloy metals in water, preserving the stoichiometry of the target metals.**

The intense research activity in the field of nanoparticles that has been conducted by chemists, physicists, and material scientists is motivated by the search for new materials in order to further miniaturize electronic devices, as well as by the fundamental question of how molecular electronic properties evolve with increasing size in this intermediate region between molecular and solid-state physics.<sup>1</sup> In particular, nanocomposites, *i.e.*, alloy and/or core–shell particles, are attractive materials because of their composition-dependent optical and catalytic properties. Papavassiliou has successfully prepared Au–Ag alloy particles *via* evaporation of Au–Ag alloys.<sup>2</sup> Liz-Marzan and Philipse prepared various bimetallic colloidal nanoparticles (Au–Ag, Au–Pt, and Ag–Pt) by reducing the metal salts in aqueous, optically transparent dispersions of inorganic fibers.<sup>3</sup> Our research group<sup>4</sup> and El-Sayed *et al.*<sup>5</sup> employed simultaneous reduction of gold and silver salts to form Au–Ag alloy particles with 4 and 18 nm diameters, respectively. Very recently, Hodak *et al.*<sup>6</sup> and Chen and Yeh<sup>7</sup> reported the production of Au–Ag alloy nanoparticles by laser irradiation of either the Au–Ag core–shell nanoparticles or the gold and silver colloidal mixtures. This suggests that the interaction between laser light and nano/colloidal particles can result in compositional changes *via* a melting process.<sup>6–8</sup> Herein, we report that homogeneous alloy nanoparticles can be produced even from bulk alloys by laser ablation in water.<sup>9</sup> A gold–silver system is chosen as a model case since both metals are miscible in all proportions in bulk due to their comparable lattice constants. Moreover, UV-vis absorption spectroscopy can readily be applied to differentiate an alloyed structure from a core–shell one for Au–Ag bimetallic particles.<sup>3–5</sup>

Initially, Au–Ag bulk alloys were prepared by inductively heating two metals at high frequency; metals used were in molar ratios of Au:Ag = 3:1, 2:2, and 1:3. Hereafter, we will refer to the metal nanoparticles prepared from the Au–Ag alloys in molar ratios of 3:1, 2:2, and 1:3 as Au<sub>0.75</sub>Ag<sub>0.25</sub>, Au<sub>0.5</sub>Ag<sub>0.5</sub>, and Au<sub>0.25</sub>Ag<sub>0.75</sub>, respectively.† Silver and gold nanoparticles are known to show plasmon absorption bands in the visible region (at ~390 and ~520 nm, respectively<sup>10</sup>). In fact, distinct peaks are observed at 394 and 518 nm in the UV-vis spectra of the Ag and Au nanoparticles prepared from pure metals (see the spectra labeled (a) and (e) in Fig. 1). In Fig. 1 are also shown the UV-vis spectra of the Au<sub>0.25</sub>Ag<sub>0.75</sub>, Au<sub>0.5</sub>Ag<sub>0.5</sub>, and Au<sub>0.75</sub>Ag<sub>0.25</sub> samples (see the spectra labeled (b), (c), and (d), respectively). Peaks are clearly observed at 427, 460, and 493 nm, respectively, for these samples; all these peaks are located at intermediate positions between the intrinsic Ag and Au plasmon bands. Hence, they must arise from the surface plasmon absorptions of alloyed nanoparticles. It is noteworthy that the plasmon absorptions of the gold–silver composite clusters are linearly red-shifted from that of a monometallic Ag cluster in proportion to the increase in the mol fraction of the Au content. This is demonstrated by Fig. 2, in which the UV-vis

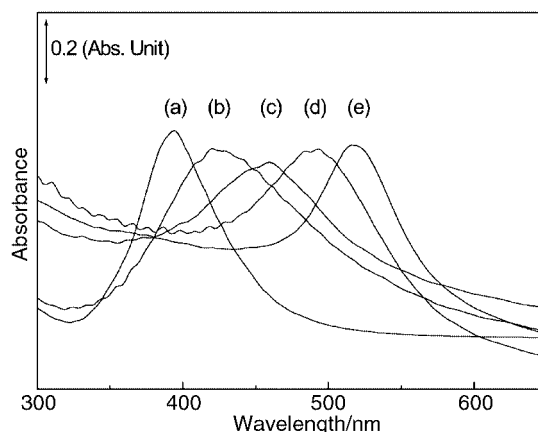


Fig. 1 UV-vis absorption spectra of Au–Ag alloy nanoparticles produced in distilled water with nominal formulae of (a) Ag, (b) Au<sub>0.25</sub>Ag<sub>0.75</sub>, (c) Au<sub>0.5</sub>Ag<sub>0.5</sub>, (d) Au<sub>0.75</sub>Ag<sub>0.25</sub>, and (e) Au.

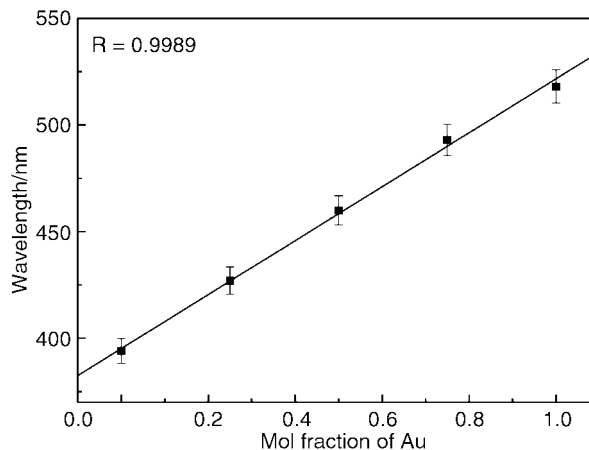
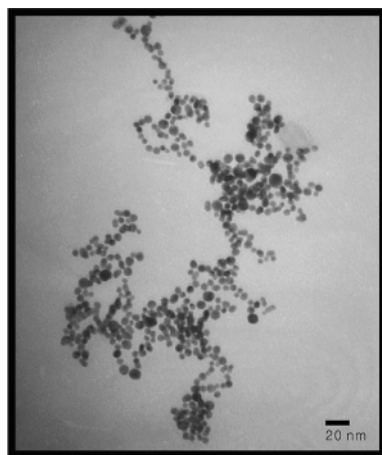


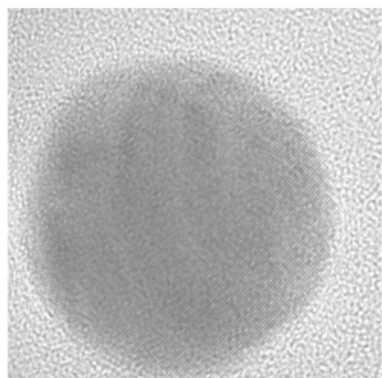
Fig. 2 Positions of surface plasmon bands plotted against the mol fractions of Au atoms in alloy nanoparticles.

absorption peak position is plotted against the mol fraction of Au in the precursor samples. Two plasmon bands would be expected if the clusters consisted of individual Au and Ag particles or of bimetallic composites with a core–shell structure.<sup>4,10</sup> All these UV-vis spectral features suggest that the Au–Ag composite particles prepared in this work are neither a simple mechanical mixture of two different monometallic particles nor bimetallic nanoparticles with a core–shell structure.

Fig. 3(a) shows a typical TEM (JEM-2000 EXII, 160 kV) image taken for a Au<sub>0.5</sub>Ag<sub>0.5</sub> sample. As can be seen in the image, most of the particles are not agglomerated and their average size is ~10 nm. Other samples showed similar TEM images. As surmised from UV-vis absorption spectroscopy, the probability of the presence of core–shell particles is proved to



(a)



(b)

**Fig. 3** (a) TEM image of Au–Ag alloy nanoparticles with a nominal formula of  $\text{Au}_{0.5}\text{Ag}_{0.5}$ . (b) HRTEM image of a 16 nm diameter Au–Ag alloy nanoparticle with a nominal formula of  $\text{Au}_{0.5}\text{Ag}_{0.5}$ .

be very low from the energy dispersive X-ray spectroscopy (EDX) analysis. In the latter analysis, peak integration and normalization were carried out to measure the Au-to-Ag ratio in individual particles, and the data were collected over 10 particles. The EDX analysis on the  $\text{Au}_{0.75}\text{Ag}_{0.25}$ ,  $\text{Au}_{0.5}\text{Ag}_{0.5}$ , and  $\text{Au}_{0.25}\text{Ag}_{0.75}$  particles thus yielded atomic ratios of Au:Ag = 75.79:24.21 ( $\pm 1.65$ ), 49.75:50.25 ( $\pm 1.01$ ), and 25.14:74.86 ( $\pm 1.71$ ), respectively. The results were always comparable to within 2%. These observations indicate that the laser-ablated products are indeed homogeneous alloyed nanoparticles.

Fig. 3(b) is a high-resolution TEM (HRTEM, JEM-3000F, 300 kV) image of the sample in Fig. 3(a). We can estimate from this image that the lattice plane spacing is about 2.35 Å. Much the same value ( $2.35 \pm 0.01$  Å) was obtained for other samples with different compositions. In fact, the value obtained herein is very close to those of pure Ag and Au, *i.e.*, 2.36 Å for Ag and 2.35 Å for Au.<sup>11</sup> This may be attributed to the fact that Ag and Au are miscible in all proportions due to their almost identical lattice constants. The unit cell size of Au–Ag alloys changes by less than 1% over the entire range from pure Au to pure Ag, and no superlattice reflections are observed in the alloys.<sup>12</sup>

Let us briefly provide a plausible mechanism for the alloyed particle formation. Immediately after the laser irradiation, the surface of a sample will reach a very high temperature by absorbing pulsed laser energy. As a consequence, atoms and/or small particles should be ejected through vaporization, followed by the build-up of a dense cloud of metal atoms (Au and Ag atoms) near the laser spot. Since the interaction between metal atoms is much greater than that between a metal atom and a

solvent molecule, the metal atom(s) will aggregate to produce nanoparticles. Since Au and Ag form nearly ideal solid solutions at all compositions,<sup>13</sup> mixing of the two metals is a thermodynamically favorable process. Therefore, nanoparticles formed must be homogeneous alloy particles.

In summary, we found that Au–Ag alloy nanoparticles could be easily produced by laser ablation of a bulk alloy in water. Formation of homogeneous alloyed particles was clearly demonstrated by UV-vis absorption spectroscopy and TEM and EDX measurements. The simplicity of the procedure is clearly a major advantage of the present method. The size distribution of nanoparticles can be readily controlled by varying the pulse energy and time of ablation. The method is versatile with respect to the kinds of metals and/or solvents employed. The absence of chemical reagents or ions in the final preparation will also be advantageous. The particles can be derivatized with suitable amphiphiles afterwards. Currently, we are attempting to synthesize other alloyed particles such as Au–Pt, Au–Cu, and Ag–Pt.

This work was supported in part by the Korea Research Foundation (KRF, 042-D00073) and the Korea Science and Engineering Foundation (KOSEF, 1999-2-121-001-5). K. K. also acknowledges KOSEF for providing a leading-scientist grant. S. W. H. was supported by KOSEF through the Center for Molecular Catalysis at Seoul National University. I.L., is a recipient of the BK21 fellowship.

## Notes and references

† For the laser ablation experiments, bulk alloys were placed at the bottom of a glass vessel filled with 10 mL triply distilled water, and then irradiated using a focused beam of a Nd:YAG laser (Continuum Surelite II-10, at 1064 nm). The typical pulse energy, repetition rate, laser pulse duration, and irradiation time were 50 mJ, 10 Hz, 6 ns, and 30 min, respectively. For reference, pure gold and silver nanoparticles were also prepared *via* the same method. Since the produced particles interfere with the subsequent laser pulses, the efficiency of the ablation process gradually decreases as a function of the irradiation time. This can be minimized by stirring the solution phase continuously during the laser ablation process. The extinction spectrum was recorded with a UV-vis absorption spectrometer (SINCO S-2130). Transmission electron microscope (TEM) images of the nanoparticles were acquired by placing drops of sample solutions on copper grids, followed by evaporation of the solvent in a vacuum desiccator.

- 1 See for example: (a) G. Schmid, *Clusters and Colloids: From Theory to Application*, VCH, Weinheim, 1994; (b) J. H. Fendler, *Nanoparticles and Nanostructured Films: Preparation, Characterization and Applications*, Wiley-VCH, Weinheim, 1998; (c) T. Sugimoto, *Fine Particles: Synthesis, Characterization, and Mechanisms of Growth*, Marcel Dekker, Inc., New York, 2000.
- 2 G. C. Papavassiliou, *J. Phys. F*, 1976, **6**, L103.
- 3 L. M. Liz-Marzan and A. P. Philipse, *J. Phys. Chem.*, 1995, **99**, 15 120.
- 4 S. W. Han, Y. Kim and K. Kim, *J. Colloid Interface Sci.*, 1998, **208**, 272.
- 5 S. Link, Z. L. Wang and M. A. El-Sayed, *J. Phys. Chem. B*, 1999, **103**, 3529.
- 6 J. H. Hodak, A. Henglein, M. Giersig and G. V. Hartland, *J. Phys. Chem. B*, 2000, **104**, 11 708.
- 7 Y.-H. Chen and C.-S. Yeh, *Chem. Commun.*, 2000, 371.
- 8 H. Kurita, A. Takami and S. Koda, *Appl. Phys. Lett.*, 1998, **72**, 789.
- 9 See for example: (a) A. Fojtik and A. Henglein, *Ber. Bunsen-Ges. Phys. Chem.*, 1993, **97**, 252; (b) M. S. Sibbald, G. Chumanov and T. M. Cotton, *J. Phys. Chem.*, 1996, **100**, 4672; (c) I. Srnová, M. Procházka, B. Vlčková, J. Štěpánek and P. Malý, *Langmuir*, 1998, **14**, 4666.
- 10 P. Mulvaney, *Langmuir*, 1996, **12**, 788.
- 11 P. Mulvaney, M. Giersig and A. Henglein, *J. Phys. Chem.*, 1993, **97**, 7061.
- 12 M. LeBlanc and W. Erler, *Ann. Phys.*, 1933, **16**, 321.
- 13 H. Okamoto and T. B. Massalki, *Binary Alloy Phase Diagrams*, ASM International, Ohio, 1990.